Tellus (1997), 49B, 72–79
Printed in UK – all rights reserved

TELLUS
ISSN 0280–6509

Contribution of sea salt aerosol to the planetary clear-sky albedo

By BARBARA WINTER* and PETR CHÝLEK *Atmospheric Science Programme, Departments of Physics and Oceanography, Dalhousie University, Halifax, Nova Scotia, B3H 4J1, Canada*

(Manuscript received 13 November 1995; in final form 3 June 1996)

ABSTRACT

In order to understand the response of the earth-atmosphere-aerosol system to climate forcing by greenhouse gases, it is essential to know the relative importance of the different factors within it. The purpose of the present work is to determine how much of the planetary clear sky albedo is due to the layer of sea salt aerosol that exists over the oceans. We calculate ΔF (the change in solar flux entering at the top of the atmosphere) due to the presence of the sea salt aerosol layer, then show that this ΔF is opposite in sign and comparable in magnitude to the predicted radiative forcing by increased levels of CO_2. Since sea salt is a stable component of the atmosphere, its radiative effects are already included in any measurement or calculation of the current planetary albedo. But when studying climates with stronger winds (leading to a greater sea salt aerosol loading), it is important to factor in the greater cooling due to sea salt, as an omission of this effect would lead to an underestimate of the planetary albedo.

1. Introduction

In the wider field of climate studies, aerosols have received much attention for a number of reasons: they may scatter light directly or they may act as cloud condensation nuclei and affect cloud albedo; they are of a variety of chemical compositions and may be strong absorbers or strong scatterers of light; their sizes span easily five orders of magnitude; they occur everywhere over the globe; they have a wide range of concentrations, and many are anthropogenically produced. In terms of sheer mass of aerosol emitted annually to the atmosphere, the human contributions still pale in comparison with natural sources, and constitute well under half of the total annual atmospheric aerosol. The strongest natural aerosol production rate is that of sea salt, at an estimated 1000 to 10000 Tg per year (or 30 to 75% of all natural aerosols) (Blanchard and Woodcock, 1980). Since the oceans cover 2/3 of the Earth's surface, production of sea salt can be called global. Our purpose in this study is to calculate the contribution sea salt aerosol makes to the current clear sky planetary albedo, and to show that this contribution is significant.

Sea salt is ejected into the atmosphere when bubbles in wind-induced whitecaps burst at the ocean surface. The ejected droplets reach a height of only a metre or so above the sea surface, but are then distributed throughout the boundary layer by the wind (Blanchard and Woodcock, 1980; Kristament et al., 1993; Toba, 1965). Depending upon the ambient relative humidity, sea salt aerosol can exist as dry or as wetted particles, or as solution droplets. Sea salt is not pure NaCl (even when completely dry), though this is the principal constituent. O'Dowd and Smith (1993), and D'Almeida et al. (1991) give detailed chemical compositions.

* Corresponding author.

2. Calculation of sea salt radiative forcing

2.1. *Atmospheric transmittance*

The difference in clear-sky shortwave flux at the top of the atmosphere between an earth-atmosphere system with albedo R, and an earth-atmosphere-aerosol system with albedo R_a is denoted ΔF, and may be obtained in the manner of Charlson et al. (1992):

$$\Delta F = -\frac{S_0}{4}(1-N_c)T_a^2\,\Delta R, \tag{1}$$

where S_0 is the solar constant, N_c the fractional cloud cover over the oceans, T_a the atmospheric transmittance above the aerosol layer, and $\Delta R = R_a - R$ is the perturbation in the planetary albedo due to the presence of the aerosol layer. When the layer is one of sea salt aerosol, then the fraction of the Earth's surface covered by the oceans, A_{ocean}, must be factored in:

$$\Delta F = -\frac{S_0}{4}(1-N_c)\,A_{ocean}\,T_a^2\,\Delta R. \tag{2}$$

ΔR, calculated as outlined in Chýlek and Wong (1995), is:

$$\Delta R = 2(1-R)^2\beta\tau_{sca} - 4R\tau_{abs}, \tag{3}$$

where β is the integrated backscattering fraction of the layer, and τ_{sca} and τ_{abs} are its scattering and absorption optical depths, respectively. Inserting this into eq. (1) gives the full expression for ΔF:

$$\Delta F = -\frac{S_0}{4}(1-N_c)\,A_{ocean}\,T_a^2 \times [2(1-R)^2\beta\tau_{sca} - 4R\tau_{abs}]. \tag{4}$$

As written, this equation calculates a monochromatic top-of-the-atmosphere (hereafter written TOA) flux difference. The broad-band ΔF we are interested in is simply the summation $\Delta F = \Sigma\Delta F_\lambda$ over spectral bands of solar radiation (from 0.3 to 4.0 μm). That range was further subdivided into 14 bands, each of these having a width of roughly 0.2 μm. This width was chosen to capture the variations in the imaginary part of the refractive index of wetted sea salt.

The task now is to replace all the variables in eq. (4) with appropriate values. Of these, S_0, N_c and A_{ocean} come straight from the literature: The spectral TOA irradiances used in this study are taken from Thekaekara (1973), but they have been adjusted to give the currently accepted value of the solar constant $S_0 = 1368$ W/m^2. The value of the cloud cover used will be 0.6 in order to be consistent with authors doing similar radiative transfer calculations (Charlson et al., 1992). The fraction of the Earth's surface covered by oceans, A_{ocean}, is calculated using the world ocean and global surface areas given in Gill (1982). An average value for sea ice area (again from Gill, 1982) was subtracted from the ocean area, and $A_{ocean} = 0.665$.

In eq. (4), $T_a^2 = T_a^{\downarrow} \cdot T_a^{\uparrow}$, where $T_a^{\downarrow}$ and $T_a^{\uparrow}$ are the downward and upward transmittances through the atmosphere, respectively. These are calculated from a model developed by Brine and Iqbal (1983). The model calculates clear-sky atmospheric transmittance, given user-specified amounts of ozone, water vapour depth and aerosol. For ozone and water vapour depth, we relied on global, annual average values as given in the current literature. We included no aerosols at this stage because we sought the transmittance of the air lying above the sea salt aerosol layer. The model was run for a solar zenith angle of 60°. Broadband results, obtained by weighting spectral transmittances by the percent of incident irradiance contained in each spectral band, are 0.72 and 0.86 for the downward and upward transmittances. The geometric mean of these is $T_a = 0.79$. This is slightly higher than in Charlson et al. (1992) T_a of 0.76, but agrees with Penner et al. (1992), who use $T_a^{\downarrow} = 0.72$ and $T_a^{\uparrow} = 0.87$, with $T_a = 0.79$.

In order to obtain the spectral albedo of the ocean surface, R, we began by calculating the spectral Fresnel reflectances of a level surface of pure water. Refractive indices of pure water came from Kou et al. (1993), Hale and Querry (1984), and Palmer and Williams (1974). On the real ocean surface, whitecaps and surface roughness act to make the albedo higher than the Fresnel value. In his study of the variation of ocean albedo with windspeed, Plass et al. (1975) gives 1.47 as the ratio of the broadband oceanic to the broadband Fresnel reflectance for a zenith angle of 60°. To obtain realistic spectral ocean albedos, the spectral Fresnel reflectances were multiplied by this factor and the results tabulated in the last column of Table 1.

The solar zenith angle-dependent quantities T_a and R were calculated for a solar zenith angle of 60°, this being a good representative of the average

Table 1. *Transmittance model parameters, for a solar zenith angle of 60°*

Band	Range (μm)	(%)	TOA	$T^{\downarrow}_{a\lambda}$	$T^{\uparrow}_{a\lambda}$	$T_{a\lambda}$	R_{Fres}	R
1.	$0.3 \leqslant \lambda \leqslant 0.5$	21.39	295.37	0.691	0.691	0.691	0.0611	0.0898
2.	$0.5 < \lambda \leqslant 0.7$	24.28	332.17	0.887	0.888	0.887	0.0594	0.0873
3.	$0.7 < \lambda \leqslant 0.9$	16.49	225.52	0.907	0.956	0.931	0.0593	0.0872
4.	$0.9 < \lambda \leqslant 1.1$	11.07	151.44	0.695	0.991	0.830	0.0587	0.0863
5.	$1.1 < \lambda \leqslant 1.35$	7.22	98.73	0.790	0.993	0.886	0.0582	0.0856
6.	$1.35 \leqslant \lambda \leqslant 1.45$	3.88	53.06	0.051	0.981	0.224	0.0576	0.0847
7.	$1.45 < \lambda \leqslant 1.75$	5.44	74.37	0.843	0.987	0.912	0.0568	0.0835
8.	$1.75 < \lambda \leqslant 1.95$	2.12	29.02	0.044	0.922	0.201	0.0554	0.0814
9.	$1.95 < \lambda \leqslant 2.1$	1.11	15.24	0.667	0.770	0.717	0.0539	0.0792
10.	$2.1 < \lambda \leqslant 2.3$	1.17	16.03	0.907	0.998	0.951	0.0518	0.0761
11.	$2.3 < \lambda \leqslant 2.5$	0.92	12.54	0.243	0.999	0.493	0.0483	0.0710
12.	$2.5 < \lambda \leqslant 2.9$	1.29	17.69	0.001	0.499	0.022	0.0340	0.0500
13.	$2.9 < \lambda \leqslant 3.3$	0.79	10.79	0.077	0.875	0.260	0.0756	0.1111
14.	$3.3 < \lambda \leqslant 4.0$	0.68	9.38	0.744	0.933	0.833	0.0696	0.1023

Column 1 identifies the spectral band; column 2 gives its wavelength range. Columns 3 and 4 list the percentage of radiation contained in each band, and the TAO irradiance in W/m^2 respectively. Downward, upward and average transmittances are in columns 5, 6 and 7. Fresnel reflectance for a surface of water are in column 8, and ocean surface reflectances in column 9. Explanations are in the text.

over all solar zenith angles. Table 1 lists the spectral TOA irradiances, transmittances and reflectances, as well as the percent radiation contained in each spectral band, and the ranges of the spectral bands themselves.

2.2. *Sea salt optical properties, size distributions*

The parameter that describes a substance in terms of its optical properties is its complex refractive index. The refractive indices used for this study stem from a variety of sources. Values for sea salt can be found in Shettle and Fenn (1979), and for NaCl, in Eldridge and Palik (1985). For water, a very complete compilation of data is available: Hale and Querry's (1984) for the region $0.3 \leqslant \lambda \leqslant 0.6$, for $0.67 \leqslant \lambda \leqslant 2.5$, the imaginary part is from Kou et al. (1993) and the real part from Palmer and Williams (1974), and Downing and Williams' (1975) for $\lambda \geqslant 2.0$. Refractive indices of dry sea salt, dry NaCl and water are shown graphically in Fig. 1; a complete listing of all refractive indices used for this work may be found in Table 1 of the Appendix in Winter (1994). For relative humidities higher than 0%, an effective refractive index of the wetted particle was calculated from the Bruggeman mixing rule (Chýlek et al., 1988).

Once Mie scattering by individual particles over a range of radii is calculated, the results are

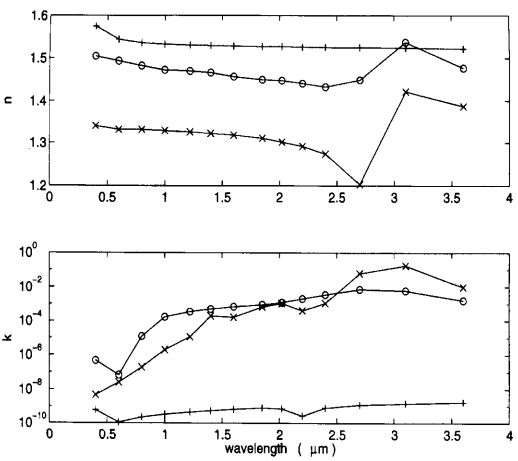

Fig. 1. Real (top; "n") and imaginary (bottom; "k") parts of the refractive index of NaCl (+), sea salt (o), and water (x). The sea salt and NaCl are dry.

integrated over a size distribution of sea salt particles. Sea salt particle sizes can be described by a log-normal distribution, characterized by the geometric mean radius r_0, the log of the standard deviation ln σ, and the total (or partial) number density N (cm^{-3}).

All manner of aerosols are commonly categorized by size or by production mechanism into three modes (or types), called either Aitken, Large and Giant, or Nucleation, Accumulation and

Coarse (WCP-55, 1983). In the literature, sea salt itself has been classified into two, sometimes all three, of these modes (WCP-55, 1983; Jaenicke, 1993; Shettle and Fenn, 1979; Blanchard and Woodcock, 1980; D'Almeida et al., 1991; Hoppel and Frick, 1990; Junge, 1972; O'Dowd and Smith, 1993). Using parameters from the literature, we calculated the mass density of sea salt in each mode, and found the values for the nucleation and coarse modes to be small compared to that of the accumulation mode. Hereafter, we will only consider sea salt aerosol ranging in size from 0.1 μm to 1.0 μm in radius, described by the accumulation mode parameters $r_0 = 0.4$ μm, $\ln \sigma = 0.3$, and $N = 20\ \mathrm{cm}^{-3}$.

The scattering and absorption by individual particles, when integrated over the size distribution, lead to the scattering and absorption coefficients k_{sca} and k_{abs}. These have dimensions of inverse length and indicate the amount of radiation removed from the incident beam as it goes a certain distance through the layer. Multiplied by the aerosol layer depth, the scattering and absorption coefficients give the scattering and absorption optical depths τ_{sca} and τ_{abs} used back in our ΔF, eq. (4). We have taken the aerosol layer depth to be 1000 m, equivalent to the depth of the turbulent mixed layer. In the solar part of the spectrum, absorption optical depths are close to zero for dry sea salt aerosol, but scattering optical depths are around 0.04. Turbulent mixing distributes the sea salt throughout the layer. The backscattering fraction of the layer, β, is approximately related to the Mie scattering asymmetry factor g (denoted G when averaged over the size distribution) by the following equation (Wiscombe and Grams, 1976):

$$\beta = \frac{1}{2}\left(1 - \frac{7}{8}G\right) \tag{5}$$

(A definition of g may be found in Bohren and Huffman (1983), p. 72). All variables in eq. (4) have now been determined.

Two other quantities, not directly related to light scattering but useful as checks of consistency with measured data, are the mass density M of the aerosol, and its production rate Q. For M, calculated using the third moment of the log-normal size distribution, we found 18 $\mu g/m^3$. This falls well into the range given by Erickson et al. (1986) in his study of sea salt aerosol mass densities over the world oceans. Our calculated production rate, using the just-stated mass density of sea salt aerosol and a layer depth of 1000 m., is 1088 Tg/yr, again within the range of production rates given in the literature (Blanchard and Woodcock, 1980; Blanchard, 1985; D'Almeida et al., 1991; Jaenicke, 1993; Pruppacher and Klett, 1978; Spillane et al., 1986; Winkler et al., 1991).

3. Results and discussion

The size distribution parameters listed in the preceding section are for dry sea salt particles, (i.e., at a relative humidity, hereafter RH, of 0%) and as such constitute only a starting point for determining more universally valid size distributions. Sea salt arrives in the air in the form of brine droplets, which evaporate until they are in equilibrium with the surrounding air. The crystallization relative humidity for NaCl droplets is close to 50% (Andrews and Larson, 1993), so that sea salt aerosol is wetted between 50% and the deliquescence RH of 75%, and dissolved when the relative humidity exceeds 75%.

Peixoto and Oort (1992) give an annual mean relative humidity of 75% for the lowest tens of metres above the ocean surface. Such a round number disguises the fact that the relative humidity can vary greatly in a space of hours; between morning and noon, for example, as the temperature increases, or following the passage of a front, or through the mixing down of drier or moister air by turbulent eddies.

The growth of aerosol particles with increasing relative humidity and the resulting change in the size distribution parameters was calculated using the Köhler equation (Pruppacher and Klett, 1978) for an equilibrium water vapour pressure over the surface of a solution droplet formed from the original dry aerosol particle. For each radius within the limits of the size distribution of the dry aerosol, we calculate the corresponding wet radius for a given relative humidity. The constraint of number conservation is imposed; there is no loss of particles due to coalescence, and no competition for the available water vapour. A size distribution (log-normal) is fitted to the number density and new range of radii, giving new values for r_0 and $\ln \sigma$.

The changes in the optical properties of the sea salt aerosol as the relative humidity is increased

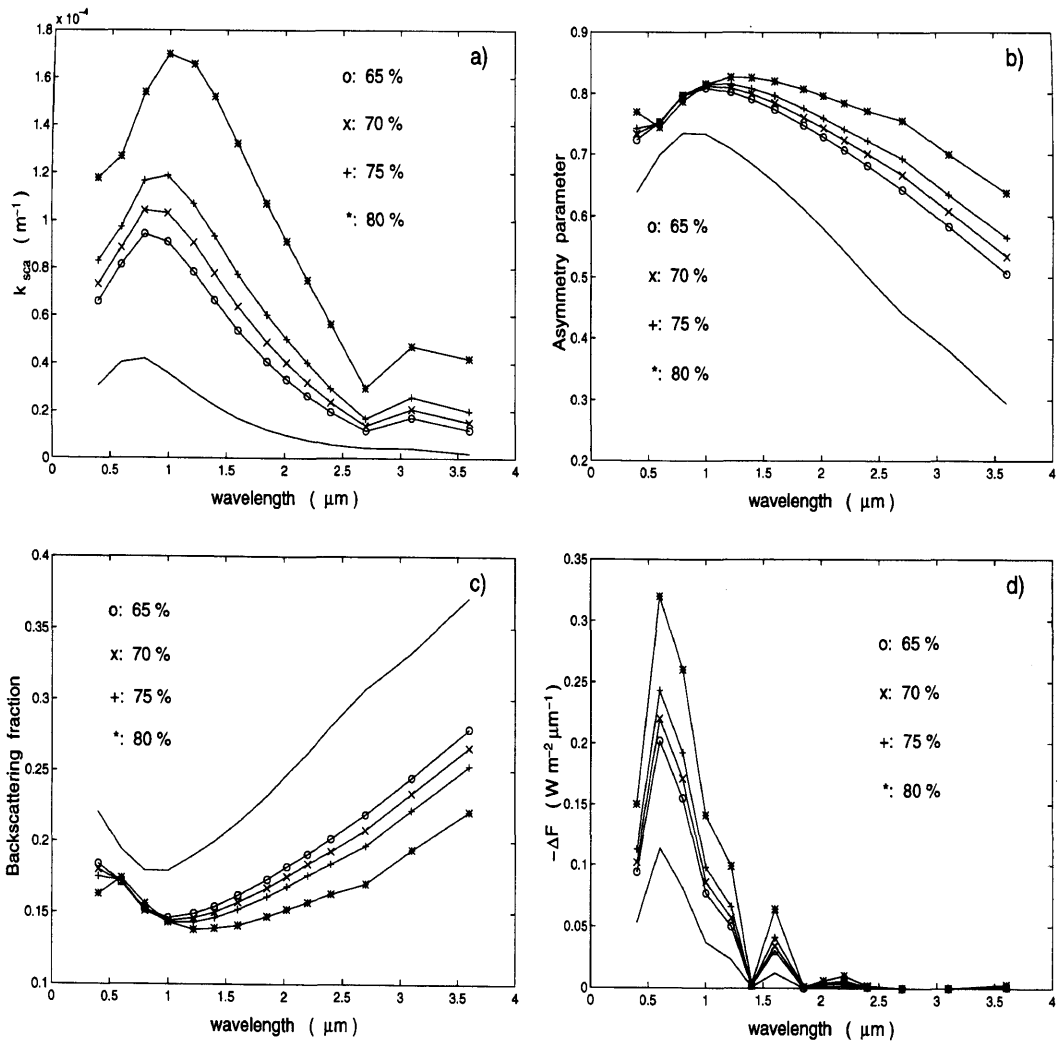

Fig. 2. Increase, for a layer of sea salt aerosol, in (a) the scattering coefficient k_{sca}, (b) the average asymmetry parameter G, (c) the average backscattering fraction β, and (d) the magnitude of ΔF_λ, as relative humidity is increased. The solid line (without symbols) is for dry sea salt; symbols give % relative humidity.

can be seen in Fig. 2. Notice that as the particles grow, scattering in the forward direction is preferred; however, because the particles are larger, the overall effect is to increase the magnitude of ΔF. The scattering optical depth, τ_{sca}, of sea salt aerosol at 75% RH is around 0.1 at solar wavelengths. Toon and Pollack report optical depths of 0.05 to 0.14 at 0.5 μm wavelengths, for measurements of marine aerosol made at all latitudes (Toon and Pollack, 1976). The highest values occur in the tropics, and optical depths in the Northern Hemisphere tend to be higher than at corresponding latitudes in the Southern Hemisphere. As mentioned above, our optical depths for a dry size distribution were 0.04. The model optical depths, then, are in agreement with measured data.

Increased RH causes the modal radius of the size distribution to grow, but has little effect on its width (as characterized by ln σ). A modification

of the prevailing windspeed, however, can influence both of these: a stronger wind, for example, would suspend not only more particles overall, but more particles in the larger end of the size spectrum, thereby widening the size distribution. In order to mimic the effect of the wind, we allowed our value of ln σ to increase from 0.3 to 0.5 and to 0.7, while maintaining the modal radius at $r_0 = 0.4$ μm. The mass density of the dry aerosol thereby rises from 18 μg/m^3 to 36 μg/m^3 and 107 μg/m^3. Results are graphed in Fig. 3. As the size distribution is widened, it includes more par-

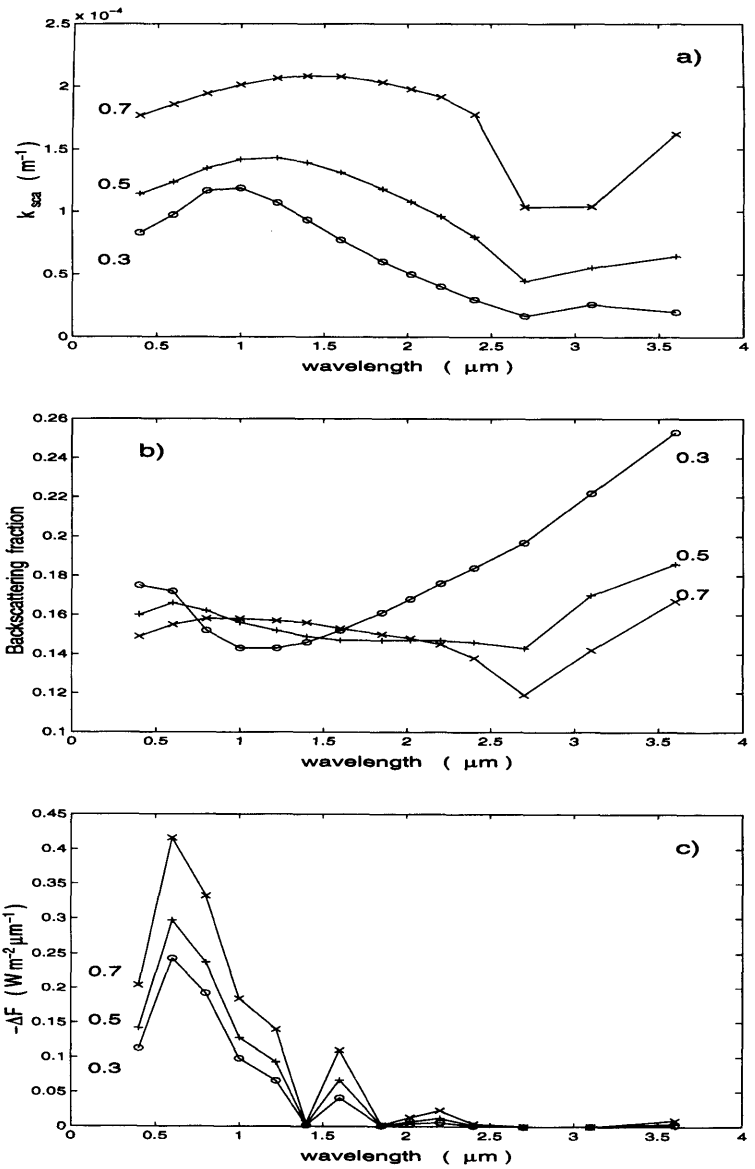

Fig. 3. The effect of changing the width of the size distribution, from ln$\sigma = 0.3$ to ln$\sigma = 0.5$ and ln$\sigma = 0.7$, on (a) the scattering coefficient k_{sca}, (b) the average backscattering fraction β, and (c) the magnitude of ΔF_λ. Relative humidity is 75%, modal radius r_0 is maintained at 0.69 μm.

ticles of larger sizes. The effect is again to reduce the fraction of radiation scattered into the backward hemisphere, but the overall amount of scattering, as characterized by k_{sca}, increases to such an extent that ΔF_λ is nonetheless greater for wide size distributions than for narrow ones. Thus stronger prevailing winds increase the cooling potential of sea salt aerosol.

The broadband values of ΔF (W/m^2) as a function of relative humidity are graphed for three size distributions in Fig. 4. The lowest values correspond to the present-day sea salt aerosol amounts, and range from $\Delta F = -0.6$ W/m^2 to $\Delta F = -2.0$ W/m^2. For the 2 wider size distributions, such as may be caused by stronger prevailing winds, ΔF extends from -1.5 W/m^2 to nearly -4.0 W/m^2. For the widest size distribution ($M =$ 107 μg/m^3), the optical depth at solar wavelengths is 0.2 when the relative humidity is 75%.

A standard of comparison is necessary before these results can be interpreted. The positive forcing caused by projected doubling of atmospheric CO_2 is about 4 W/m^2. That caused by the increase of CO_2 since the advent of the industrial era is about 1.25 W/m^2 (Charlson et al., 1992). In magnitude, then, the "cooling" due to sea salt aerosol is significant with respect to this yardstick, even at low relative humidities. At 75%, it is close to radiative forcing attributed to the increase in atmospheric CO_2 since the beginning of the industrial age. Clearly the reduction in incident solar flux caused by sea salt aerosol is important and must be recognized. In the current climate, it is of course already included in the planetary albedo, being an essentially invariant (on average) atmospheric constituent. However, the ice core record shows increases in sea salt aerosol deposited at high latitudes during the Younger Dryas (Mayewski et al., 1993). This suggests stronger mean prevailing winds than in the present (to cause the higher loadings of sea salt in the atmosphere). When modelling such a climate, it is important to include the appropriate contribution to the planetary albedo made by sea salt aerosol.

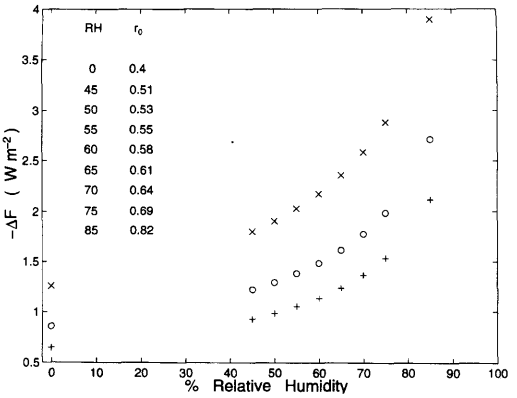

Fig. 4. Radiative forcing as a function of relative humidity for three size distributions of sea salt aerosol: (+) $M = 18$ μg/m^3, $\ln\sigma = 0.3$, (o) $M = 36$ μg/m^3, $\ln\sigma = 0.5$, and (x) $M = 107$ μg/m^3, $\ln\sigma = 0.7$. The modal radius varies with relative humidity but is held the same for all three size distributions. Values are listed in the figure. RH in %, r_0 in μm.

4. Conclusion

The purpose of this study has been to determine how much of the planetary albedo is due to the layer of sea salt aerosol that exists over the oceans. We found the global and annual average radiative forcing for sea salt aerosol in an environment of 70 to 85% RH to be up to -2.0 W/m^2. That number doubles as wider size distributions of sea salt aerosol are considered. Further, if we consider a localized case with overhead incidence of solar radiation and no clouds (instead of an annual, global average), the magnitude of ΔF falls into the range -6 to -10 W/m^2. The contribution of sea salt aerosol to the planetary albedo is non-negligible in the current climate, and becomes very important in climates with stronger winds.

5. Acknowledgments

The authors wish to express their thanks to Peter Damiano and Jeff Wong for their help with the programming, and to Dr. Qiang Fu for his useful comments upon reading the manuscript. Dr. Eric Shettle's suggestions on references for refractive indices are gratefully acknowledged. This research was funded in part by grants from the AES and NSERC.

REFERENCES

Andrews, S. and Larson, S. M. 1993. Effect of surfactant layers on the size changes of aerosol particles as a function of relative humidity. *Environ. Sci. Tech.* **27**, 857–865.

Blanchard, D. C. 1985. The oceanic production of atmospheric sea salt. *J. Geophys. Res.* **90**(C1), 961–963.

Blanchard, D. C. and Woodcock, A. H. 1980. The production, concentration and vertical distribution of the sea-salt aerosol. *Ann. N.Y. Acad. Sci.* **338**, 330–347.

Bohren, C. and Huffman, D. R. 1983. *Absorption and scattering of light by small particles.* Wiley, New York.

Brine, D. T. and Iqbal, M. 1983. Diffuse and global spectral irradiance under cloudless skies. *Solar Energy* **30**, 447–453.

Charlson, R. J., Schwartz, S. E., Hales, J. M., Cess, R. D., Coakley, Jr., J. A., Hansen, J. E. and Hofman, D. J. 1992. Climate forcing by anthropogenic aerosols. *Science* **255**, 423–430.

Chýlek, P., Srivastava, V., Pinnick, R. G. and Wang, R. T. 1988. Scattering of electromagnetic waves by composite spherical particles: Experiment and effective medium approximations. *Appl. Opt.* **27**(12), 2396–2404.

Chýlek, P. and Wong, J. 1995. Effect of absorbing aerosols on the global radiation budget. *Geophys. Res. Letters* **22**, 929–931.

D'Almeida, G. A., Koepke, P. and Shettle, E. P. 1991. *Atmospheric aerosols, global climatology and radiative characteristics.* A. Deepak Publishing, Hampton, VA.

Downing, H. D. and Williams, D. 1975. Optical constants of water in the infrared. *J. Geophys. Res.* **80**, 1656–1661.

Eldridge, J. E. and Palik, E. D. 1985. Sodium chloride. In: *Handbook of optical constants of solids* (ed. E. D. Palik). Academic Press, Inc., Orlando, Florida, 775–793.

Erickson, D. J., Merrill, J. T. and Duce, R. A. 1986. Seasonal estimates of global atmospheric sea-salt distributions. *J. Geophys. Res.* **91**(D1), 1067–1072.

Gill, A. E. 1982. *Atmosphere-ocean dynamics*, vol. 30, International Geophysics Series. Academic Press.

Hale, G. M. and Querry, M. R. 1984. Optical constants of water in the 200 nm to 200 μm wavelength region. *Appl. Opt.* **23**, 1206–1225.

Hoppel, W. A. and Frick, G. M. 1990. Submicron aerosol size distributions measured over the tropical and south pacific. *Atmos. Environ.* **24A**, 645–659.

Jaenicke, R. 1993. Tropospheric aerosols. In: *Aerosol-cloud-climate interactions* (ed. P. Hobbs). Academic Press, Inc., San Diego.

Junge, C. E. 1972. Our knowledge of the physicochemistry of aerosols in the undisturbed marine environment. *J. Geophys. Res.* **77**, 5183–5200.

Kou, L., Labrie, D. and Chýlek, P. 1993. Refractive indices of water and ice in the 0.65 to 2.5 μm spectral range. *Appl. Opt.* **32**, 3531–3540.

Kristament, I. S., Liley, J. B. and Harvey, M. J. 1993. Aerosol variability in the vertical in the southwest pacific. *J. Geophys. Res.* **98** (D4), 7129–7139.

Mayewski, P. A., Meeker, L. D., Whitlow, S., Twickler, M. S., Morrison, M. C., Alley, R. B., Bloomfield, P. and Taylor, K. 1993. The atmosphere during the younger dryas. *Science* **261**, 195–197.

O'Dowd, C. D. and Smith, M. H. 1993. Physiochemical properties of aerosols over the northeast atlantic: Evidence for windspeed-related submicron sea-salt production. *J. Geophys. Res.* **98** (D1), 1137–1149.

Palmer, K. F. and Williams, D. 1974. Optical properties of water in the near infrared. *J. Opt. Soc. Am.* **64**, 1107–1110.

Peixoto, J. P. and Oort, A. H. 1992. *Physics of climate.* American Institute of Physics, New York.

Penner, J. E., Dickinson, R. E. and O'Neill, C. A. 1992. Effects of aerosol from biomass burning on the global radiation budget. *Science* **256**, 1432–1433.

Plass, G. N., Kattawar, G. W. and Guinn, J. A. 1975. Radiative transfer in earth's atmosphere. *Appl. Opt.* **14**, 1924.

Pruppacher, H. R. and Klett, J. D. 1978. *Microphysics of clouds and precipitation.* D. Reidel Publishing Co., Dordrecht.

Shettle, E. P. and Fenn, R. W. 1979. *Models for the aerosols of the lower atmosphere and the effects of humidity variations on their optical properties.* Environmental Research Paper no. 675 NTIS ADA 085951, AFGL-TR-79-0214.

Spillane, M. C., Monahan, E. C., Bowyer, P. A., Boyle, D. M. and Stabeno, P. J. 1986. Whitecaps and global fluxes. In: *Oceanic whitecaps and their role in air-sea exchange processes* (eds. E. C. Monahan and G. MacNiocaill). D. Reidel Publishing Co., Dordrecht.

Thekaekara, M. P. 1973. Solar energy outside the earth's atmosphere. *Solar Energy* **14**, 109–127.

Toba, Y. 1965. On the giant sea-salt particles in the atmosphere, Part I. *Tellus* **17**, 131–145.

Toon, O. B. and Pollack, J. B. 1976. A global average model of atmospheric aerosols for radiative transfer calculations. *J. Appl. Met.* **15**, 225–246.

WCP-55 1983. *Report of the expert meeting on aerosols and their climatic effects.* World Climate Programme, World Meteorological Organization, Geneva.

Winkler, T., Goschnik, J. and Ache, H. J. 1991. Reactions of nitrogen oxides with NaCl as model of sea salt aerosol. *J. Aerosol Sci.* **22**(suppl. 1), S 605–S 608.

Winter, B. 1994. *Light scattering by a sea salt aerosol layer.* MS thesis. Dalhousie University, Halifax, Canada.

Wiscombe, W. J. and Grams, G. W. 1976. The backscattered fraction in two-stream approximations. *J. Atmos. Sci.* **33**, 2440–2451.